

Lawrence Berkeley National Laboratory

Lawrence Berkeley National Laboratory

Title

Femtosecond x-ray detectors via optical gating

Permalink

<https://escholarship.org/uc/item/7fd3h8hn>

Author

Glover, T.E.

Publication Date

2001-06-28

Femtosecond x-ray detectors via optical gating

T.E. Glover

Advanced Light Source Division, Lawrence Berkeley National Laboratory

Berkeley, CA 94720

ABSTRACT

Progress in ultrafast x-ray science demands a new generation of high time-resolution x-ray detectors. We discuss an x-ray and laser cross-correlation technique which could serve as a basis for a femtosecond x-ray detector. The cross-correlation technique is based on visible-laser-induced modifications to x-ray photoelectron spectra.

INTRODUCTION

Recent advances in ultrafast (picosecond and femtosecond) x-ray sources offer the promise of directly probing the fast atomic motion which drives dynamical processes (chemical reactions, phase transitions etc.) important to physics, chemistry and biology¹. These ultrafast shortwavelength sources impose new demands on x-ray detector technology. The most mature ultrafast x-ray detectors are currently specialized x-ray streak cameras. These devices (with demonstrated time resolution of 2 ps in 1990) offer time-resolution of about one-half of a picosecond^{2,3}. While impressive progress has been made in x-ray streak camera technology, there are significant obstacles to reaching even 100 fs time-resolution and fundamental limits^{2,3} inherent to this approach make it doubtful that 1-10 fs resolution could be reached in the foreseeable future.

Accordingly, it is fitting to assess other approaches to the development of femtosecond x-ray detectors. A similar need for high time-resolution detectors faced the visible spectroscopy community upon the development of picosecond and femtosecond lasers. The solution was to utilize non-linear optical processes as a basis for developing high time-resolution detectors. In laser spectroscopy, optical-optical nonlinear processes provide unparalleled time resolution while also providing a basis for a broader range of diagnostic technologies⁴. We discuss extension of these nonlinear techniques to the x-ray regime through a consideration of an x-ray and laser cross-correlation technique. The technique is based on laser-induced modifications to x-ray photoelectron spectra and can be used as a basis for a femtosecond x-ray detector. The time-resolution of such a detector would be limited only by the duration of a short laser pulse (currently < 10 fs).

OPTICAL GATING

An x-ray and laser cross-correlation technique can be based on laser induced modifications to x-ray photoelectron spectra (XPS). The comparative simplicity of this approach is evidenced by the fact that initial demonstrations of the technique^{5,6} yielded time-resolution (50 fs, Figure 1 inset) nearly an order of magnitude better than what is currently obtained with competing technologies². While this (and indeed all two-color) technique(s) relies on a femtosecond laser system, this is not an overly restrictive requirement since the majority of femtosecond experiments are of the pump-probe variety; a femtosecond laser system is already available to trigger the material dynamics of interest.

Photoelectron-based techniques which rely on bound-free x-ray transitions enjoy an advantage over schemes employing bound-bound transitions. The bound-free transitions are not resonant transitions so that subsequent measurement techniques can be applied to a broad range of x-ray wavelengths. With regard to time-resolution, photoelectron techniques are intrinsically high-time-resolution since the x-ray photoelectron must (in order to conserve momentum) be in the vicinity of the nucleus (of order a Bohr radius) to exchange energy with the laser field. Even relatively slow electrons (~ 1 eV) move away from the nucleus rapidly ($6\text{\AA}/\text{fs}$) so that the intrinsic time-resolution of the process is fast and the laser duration sets the practical time-resolution achievable.

Below we consider two regimes of laser-induced XPS modifications : (1) moderate laser intensity (roughly 10^9 W/cm²- 10^{13} W/cm²) where we consider scattering of laser photons by the x-ray photoelectron and (2) the limit of high laser intensity and long laser wavelength where the electron-laser interaction is treated assuming a classical laser field⁸.

Continuum Scattering

At moderate laser intensity ($<10^{14}$ W/cm²) scattering of laser photons by the x-ray photoelectron is the primary XPS modification. The underlying physical principles were demonstrated more than two decades ago in experiments by Weingartshofer *et al.*⁷ on laser-assisted electron scattering. In those experiments monoenergetic electrons were scattered from an atom placed within a laser field. The electrons emerged from the scattering target with a spectrum of energies : the initial energy and additional peaks spaced from the initial energy-peak by integer multiples of the laser photon energy. The electron energy was modified due to scattering (absorption and/or emission) of laser photons.

The extension of these ideas to x-ray photoionization in a laser field was (to our knowledge) first demonstrated by Schins *et al* at Centre d'Etudes de Saclay⁵ and by our group at the Berkeley National Laboratory⁶. In the Berkeley experiments, soft x-rays (~ 40 eV) were used to photoionize a helium gas sample. Photoelectron spectra were measured using a time-of-flight electron spectrometer (Fig. 1, dashed line) and were perturbed with a femtosecond laser pulse. The laser-perturbed photoelectron spectrum (Fig. 1, solid line) exhibits additional peaks due to scattering of laser photons. This laser-assisted photoelectric effect can be thought of as half an electron scattering event . The x-

ray photon projects a (formerly bound) electron into the laser field and this electron (while in the vicinity of the nucleus) scatters laser photons.

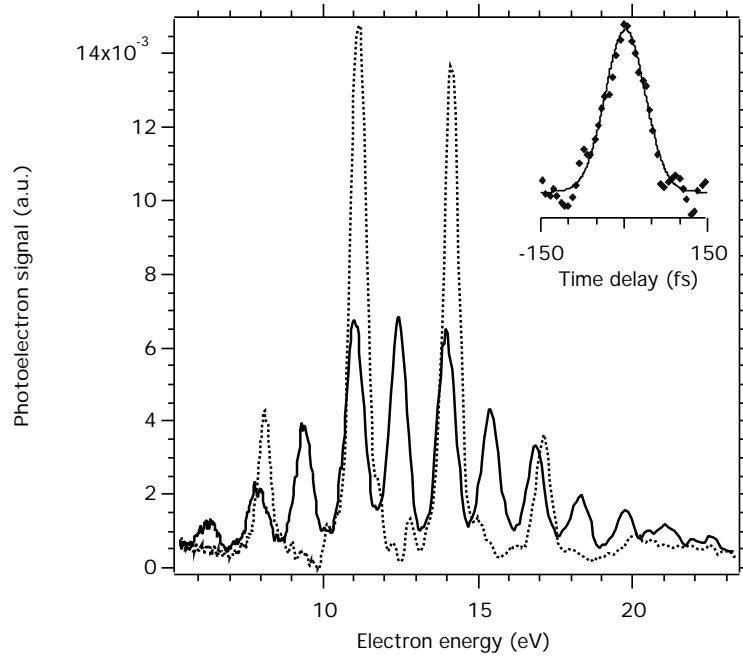


Figure 1. Experimental results demonstrating optical scattering. Soft x-rays (four high-order laser harmonics) at ~ 40 eV photoionize a He gas sample producing an ‘unperturbed’ photoelectron spectrum (dashed line). When the soft x-ray photoionization event occurs in the presence of a femtosecond laser pulse (800 nm, $\sim 10^{12}$ W/cm 2) additional peaks appear due to scattering of laser photons (solid line). By measuring the amplitude of an optical scattering peak vs soft x-ray/laser relative arrival time at the He sample, a soft x-ray/laser cross-correlation curve is obtained (inset shows a cross-correlation between a 70 fs laser pulse and a 50 fs soft x-ray pulse).

We mention that a second effect accompanies laser-assisted x-ray photoionization : the XPS is shifted to lower energy due to a laser-induced AC stark shift of the continuum. The AC stark shift is equal in magnitude to the time-averaged energy of a free-electron in the laser field, $e^2E^2/4m^2$, a quantity often called the laser ponderomotive potential (E is the laser field strength, ω the laser frequency, m and e are the electron mass and charge). The ponderomotive potential is numerically equal to ~ 1 eV for a laser wavelength of 1 μm and a laser intensity of 10^{13} W/cm 2 . As discussed below, optical scattering typically requires lower laser intensity so that it is easy to work in a regime where stark shifts are negligible.

Requirements on X-ray Spectral Bandwidth

In optical scattering one observes peaks spaced from the primary (unperturbed) x-ray peak by integer units of the optical photon energy. Background-free detection of the optical scattering sidebands requires a spectrally narrow unperturbed photoelectron peak (one whose bandwidth is narrower than ‘ n ’ units of the laser photon energy; ‘ n ’ is the number of scattered optical photons). This requirement for efficient (i.e. background free) observation of optical sidebands implies two conditions. First, the natural width associated with the bound-free transition should be ‘narrow’ (as specified above). This implies that (at short x-ray wavelength) it may be preferable to look for sidebands near M

or L shell primary electrons rather than near K shell electrons (lower yield but also narrower peaks and accordingly lower background). As a second condition, one prefers a spectrally narrow x-ray source. If, however, it is inconvenient to extract a spectrally narrow portion of the target x-ray pulse then one can imagine exercising one of several options.

First, one can frequency up-convert the laser photons to higher energy so that the sidebands are further displaced from the primary electron peak. The disadvantage of this solution is that the optical-sideband-amplitude will be decreased as a result of two factors : (1) non-unity up-conversion efficiency of the laser light and (2) reduced optical scattering efficiency at shorter laser wavelength. With respect to the second point, if one is operating in a regime where the optical scattering scales linearly with laser intensity, then the scattering efficiency decreases rapidly with decreased laser wavelength (approximately as wavelength to the fourth power); it is less efficient to work at short laser wavelength.

Second, one can use a thin-foil to create a sharp edge in the transmitted x-ray spectrum. Foil transmission edges are sufficiently sharp on the scale of a few eV to make this approach feasible if the x-ray spectrum overlaps a known/convenient foil transmission edge.

Third, one can detect Auger electrons rather than primary electrons. Auger emission in the presence of a laser field has been demonstrated by Schins *et al*⁵; optical sidebands are also observed near the Auger electron peak. This is an attractive option if the Auger width of interest is narrower than the x-ray pulse bandwidth.

Finally, if the above options are unsatisfactory, one can abandon background-free detection at the expense of increased data acquisition time. We note that if a signal sits on top of a background which is N times larger than that signal, then the data acquisition time required to achieve a fixed signal-to-noise ratio increases by a factor of 1+N. Given that reasonable scattering efficiencies can be obtained (~10-50%), this is a reasonable approach as long as the x-ray pulse length is not too much longer (several orders of magnitude) than the desired time-resolution (set by the laser duration). If the x-ray pulse is much longer than the laser pulse then one is looking for a small fractional effect and the increased data acquisition time can be prohibitive.

We note that constraints on the x-ray pulse spectrum are not a significant limitation for source characterization (i.e. measuring femtosecond pulses; one of the above options can be used) but may be problematic in spectroscopic applications where one wants parallel data collection over a broad (x-ray) spectral range. In this case it is preferable to work in a limit where electron energy modulations can be large compared to the laser photon energy. This large-energy-modulation limit is considered for moderate laser intensity in the next section (multiple continuum scattering) and for high intensity in the following section ('classical limit').

Scattering efficiency and required Laser Power

Simulations of the optical scattering process are in good agreement with measured data⁶ and indicate that the optical scattering probability, P_n , can be written as⁶ :

$$P_n = (3/2) \cdot (p/p_0)^3 \cdot \left[\frac{1 + (a/\hat{O})^2 \cdot p_0^2}{1 + (a/\hat{O})^2 \cdot p^2} \right]^4 \cdot \int_0^\pi \sin(\theta) \cdot \cos^2(\theta) J_n^2(\dots) d\theta \quad (1)$$

In (1), P_n is the probability that the photoelectric effect is accompanied by absorption ($n>0$) or emission ($n<0$) of n laser photons, a is the Bohr radius divided by the nuclear charge; \hbar is Planck's constant divided by 2π ; the momenta, p_0 and p , are $p=[2m(\hbar k_x + n\cdot\hbar k - E_b - U_p)]^{0.5}$ and $p_0=[2m(\hbar k_x - E_b)]^{0.5}$ where m is the electron mass, $\hbar k_x$ is the x-ray photon energy, $\hbar k$ is the laser photon energy, E_b is the field free binding energy and U_p is the ponderomotive potential of the laser. The function, $J_n(x)$, is the generalized Bessel function¹⁰ and its arguments are $x = e\cdot A_0\cdot p\cdot\cos(\theta)/(m\hbar c)$, $\theta = -U_p/2\cdot\hbar k$ where e is the electron charge and A_0 is the vector potential of the laser.

Equation (1) indicates that relatively modest laser powers are required to observe optical scattering. The probability for first and second order scattering is shown in Fig. 2 (for 1 μm wavelength) and indicates that a 25% (first-order) scattering probability can be obtained using a laser intensity of 2×10^{10} W/cm^2 and 100 eV photoelectrons. The scattering process scales favorably with x-ray energy : a 25% scattering probability requires a lower laser intensity (2×10^9 W/cm^2) for 1 KeV photoelectrons. Specifically, the scattering probability (for probabilities below $\sim 25\%$) scales as the product of the laser intensity and the (laser-field-free) photoelectron energy. Accordingly, if one considers ionization from a fixed core-state, higher x-ray energy translates to higher photoelectron energy and therefore less required-laser-power. While success^{5,6} in modeling the interaction at soft x-ray wavelengths is encouraging, extension of the technique to the hard x-ray regime must be demonstrated.

The saturation behavior of the optical scattering process is also an important consideration since saturation effects will alter a two-color cross-correlation. The manner in which first and second order optical scattering saturates is shown in Fig. 2 (inset). In constructing the figure, we have calculated the probability for scattering (absorbing or emitting) one laser photon as a function of laser intensity. Calculated optical scattering probabilities are then parameterized by a power law dependence upon laser intensity (scattering probability $\sim I^q$; I =laser intensity, q =a parameter). The power-law exponent, q , therefore represents the effective non-linearity for optical scattering. This effective non-linearity changes with laser intensity (or equivalently with optical scattering probability) and represents whether a laser/x-ray cross-correlation is performed in a linear ($q\sim 1$) or saturated ($q\ll 1$) regime. Inspection of Fig. 2 (inset) illustrates that a 10% (first order) optical scattering probability giving an effective non-linearity of ~ 0.9 . This is a modest level of saturation and corresponds to an effective laser-pulse broadening of $\sim 10\%$ ($\tau_{\text{laser}}/0.9 = 1.09\tau_{\text{laser}}$; assuming a gaussian laser pulse).

Next we consider high-order continuum scattering. This is important for applications where the x-ray spectral bandwidth is not small compared to the laser photon energy. In this regime the x-ray photoelectron scatters many optical photons leading to large (tens of eV's) photoelectron peak-shifts. Continuum scattering is fairly easily saturated since the approximately free x-ray photoelectron offers little resistance to the optical field. Accordingly one can observe very high order scattering processes (10^{th} or 20^{th} order) with reasonable efficiency. In Figure 3 we show results of calculated, using Eq. (1), scattering probabilities out to 20^{th} order for a laser-field-free photoelectron energy of 100 eV, and a 1 μm laser at 2×10^{13} W/cm^2 . We see that high-order scattering probabilities of a few percent are obtained.

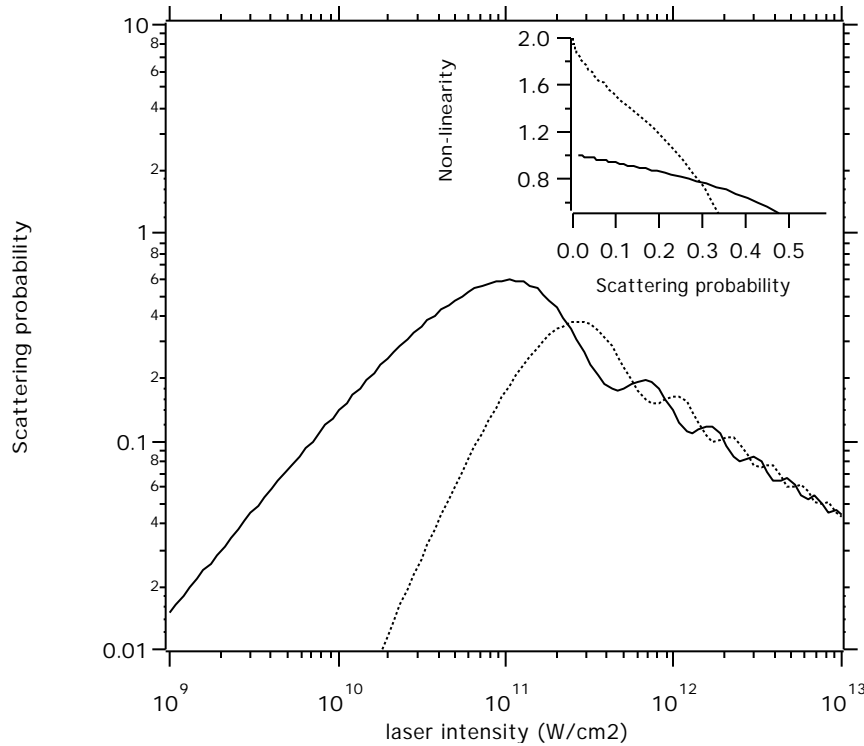


Figure 2. Calculation of optical scattering probabilities as a function of laser intensity. A 1 μm laser is assumed as are 100 eV (unperturbed) x-ray photoelectrons. The probabilities for scattering (absorbing or emitting) one (solid line) and two (dashed line) laser photon(s) are shown. The inset shows the corresponding effective non-linearities (for the optical scattering process) vs scattering probability; first (solid line) and second (dashed line) order scattering are shown. The effective non-linearity is defined as the power law dependence of the scattering process on laser intensity (see text).

Finally we mention that the laser power necessary for optical scattering is sufficiently modest as to permit high-repetition-rate operation if micro-focused x-ray beams (1-10 μm spot size) are used in combination with femtosecond laser oscillators (running at ~ 100 MHz repetition rate). For instance, a 10 fs, 5 nJ laser pulse focused to a 5 μm spot produces a peak laser intensity of $5 \times 10^{12} \text{ W/cm}^2$; this intensity is more than sufficient to observe optical scattering. For measurements and/or experiments which can operate at ~ 100 MHz repetition rate, the combination of micro-focused beams and femtosecond oscillators is attractive since this approach makes efficient use of the available x-ray flux at synchrotron light sources (which operate at high repetition rate).

Classical Limit : High Laser Intensity and Long Laser Wavelength

A second view of two-color photoelectron-based measurement techniques arises by considering the laser/electron interaction in the limit of high laser intensity and long laser wavelength. Here the ponderomotive potential (U_p) of the laser is large compared to the laser photon energy; the number of laser photons is large and one treats the electron-laser interaction classically⁹.

In this classical limit, the energy imparted to the x-ray photoelectron by the laser is determined by where in the laser field the electron is born. If the laser field is linearly

polarized then the (laser-induced) energy modulation depends on both the instantaneous laser intensity and on the laser optical phase at the moment of electron birth (x-ray photoionization). Since the electron energy changes for electrons born at different points in the laser optical cycle, laser-induced energy modulations have been proposed as a method for measuring sub-femtosecond x-ray pulses¹¹.

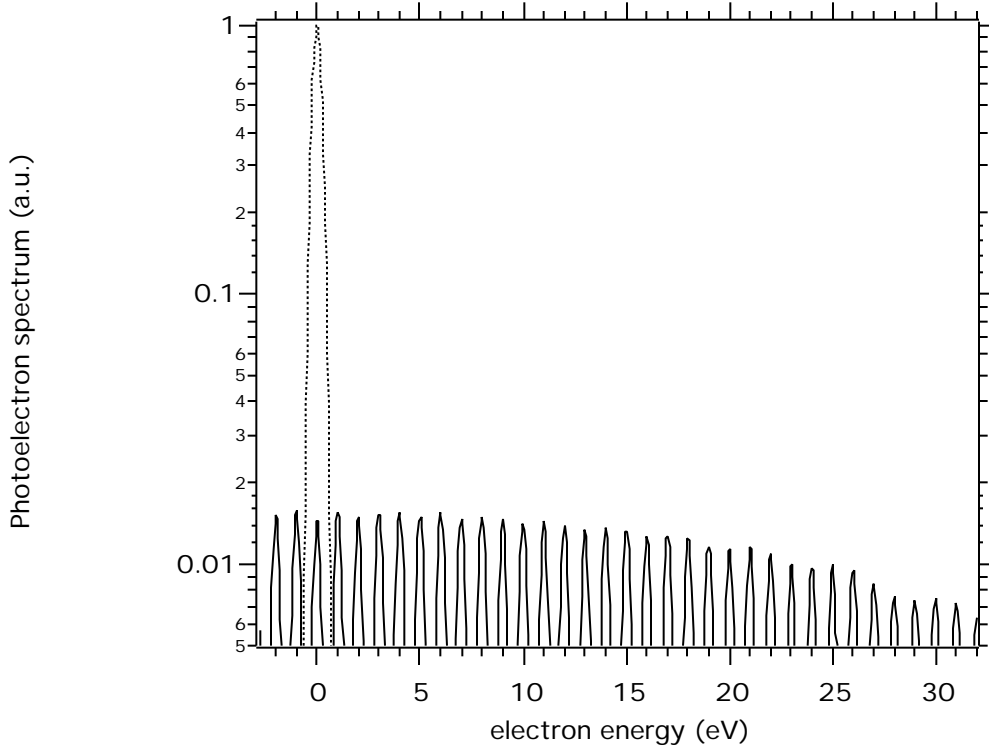


Figure 3. Calculation of high-order continuum scattering for 100 eV (unperturbed) x-ray photoelectrons. The photoelectron yield is shown as a function of relative (relative to the laser-field-free case) photoelectron energy. A photoelectron peak widths of 0.5 eV is assumed and calculations are shown for the case of no laser (dashed line) and a 1 μm laser at $2 \times 10^{13} \text{ W/cm}^2$ (solid line).

Perhaps more relevant for measurement of multi-femtosecond x-ray pulses is the electron interaction with a circularly polarized laser pulse. Here the energy modulation depends only on the instantaneous laser intensity at the moment of x-ray ionization^{9,10}. In particular, the energy kick imparted to the x-ray photoelectron by the laser pulse is equal to twice the instantaneous ponderomotive potential of the laser at the moment of electron birth. Given a femtosecond x-ray pulse and a circularly polarized laser pulse with a leading/trailing edge duration comparable to or longer than the x-ray duration, the spectrum of laser modulated electron energies constitutes a direct measure of the x-ray pulse duration. For instance, consider a 1 μm , 100 fs, circularly polarized laser pulse focused to $5 \times 10^{14} \text{ W/cm}^2$. For purposes of estimation, we assume a linear variation of laser intensity with time and approximate the ponderomotive gradient as $2U_p$ at the peak of the laser pulse divided by the laser pulse duration. The ponderomotive gradient is therefore $\sim 100 \text{ eV}/100 \text{ fs}$ or 1 eV/fs . Electrons born in the middle of the laser rising edge receive a $\sim 50 \text{ eV}$ energy kick while electrons born earlier/later receive smaller/larger energy kicks. Electrons ionized due to a 10 fs x-ray pulse would produce an $\sim 10 \text{ eV}$ wide

energy peak displaced ~ 50 eV from the laser-field-free energy peak. The laser intensity can be adjusted to modify both the energy kick and width (both are linear in the laser intensity). For target laser intensities in the range 10^{15} - 10^{16} W/cm² (maximum energy kicks of 100-1000 eV for 1 μ m, 100 fs, 1 mJ laser pulses) the required x-ray spot diameter (matched to the laser spot size) is ~ 40 μ m.

Pulse measurements in this classical limit are attractive since (as shown above) the ponderomotive energy kick can be much larger than the optical photon energy; this mitigates problems with applying photoelectron techniques to broadband x-ray sources. Similar measurement scenarios can be based on laser modifications to the angular distribution of emitted photoelectrons¹⁰. While the required laser intensities for these classical effects are not particularly high given present femtosecond lasers, the intensities are sufficiently high as to favor the use of gas-phase targets over solid targets (which will suffer ablation).

SUMMARY

In summary, the development of high time-resolution x-ray detectors is important to progress in ultrafast x-ray spectroscopy. These detectors can be used for performing fast spectroscopy and will play an important role in developing and utilizing future short-pulse light sources. With respect to this last point, two-color detectors can be used to circumvent problems with x-ray/laser synchronization at future light sources. For instance, x-ray free electron lasers are projected to produce femtosecond pulses but will not be inherently synchronized to short laser pulses which may be needed to trigger the dynamics of interest in pump-probe experiments. Phase-locking or other techniques may permit synchronization down to some fraction of a picosecond but have not been demonstrated at the sub-100 fs regime. One could circumvent this problem by using a femtosecond x-ray detector to measure the x-ray/laser time delay for each pump-probe pulse pair (the delay will vary from shot to shot providing a range of (recorded) pump-probe time delays).

ACKNOWLEDGEMENTS

This work is supported by the Department of Energy under contract AC03-76SF00098.

REFERENCES

1. Barbara, P.F., Fujimoto, J.G., Knox, W.H., & Zinth, W (eds) (1996), *Ultrafast Phenomena X*, Springer-Verlag, Berlin (1996).
2. Chang, Z., Rundquist, A., Zhou, J., Murnane, M. M., Kapteyn, H. C., Liu, X., Shan, B., Liu, J., Niu, L., Gong, M., & Zhang, X. (1996), *App. Phys. Lett.* **69**, 133-135; Gallant, P., Forget, P, Dorchie, F, Jiang, Z, Kieffer, JC, Jaanimagi, PA, Rebuffie, JC, Goulmy, C, Pelletier, JF, & Sutton, M. (2000), *Review of Scientific Instruments* **71**, 3627-3633.
3. Murnane, M.M., Kapteyn, H.C., & Falcone, R.W. (1990), *Appl. Phys. Lett.* **56** 1948-1950.
4. DeLong, K.W., Trebinio, R, & Kane, D.J. (1994), *J. Opt. Soc. Am. B* **11**, 1595-1608; Elsaesser, T., Fujimoto, J.G., Wiersma, D.A., & Zinth, W. (1998), *Ultrafast Phenomena*

XI, Springer-Verlag, Berlin.

5. Schins, J.M., Breger, P, Agostini, P, Constantinescu, R.C., Muller, H.G., Grillon, G., Antonetti, A., Mysyrowicz, A. (1994), Phys. Rev. Lett. **73**, 2180-2183; Bouhal, A., Salieres, P, Breger, P, Agostini, P, Hamoniaux, G, Mysyrowicz, A, Antonetti, A, Constantinescu, R, & Muller, HG. (1998), Phys. Rev. A **58**, 389-399.
6. Glover. T.E., Schoenlein, R.W., Chin, A.H., & Shank, C.V., (1996), Phys. Rev. Lett. **76**, 2468-2471.
7. Weingartshofer,A., Holmes, J. K., Caudle, G., & Clarke, E. M. (1977), Phys. Rev. Lett. **39**, 269-270.
8. Reiss, Howard R. (1980), Phys. Rev. A **22**, 1786-1796.
9. Corkum, P.B., Burnett,, N. H., & Brunel,F. (1989), Phys. Rev. Lett. **62**, 1259-1262.
10. Constant, E., Taranukhin, VD, Stolow, A, & Corkum, PB (1997), Phys. Rev. A **56**, 3870-3878.